



# Genetic and hormonal factors modulate spreading depression and transient hemiparesis in mouse models of familial hemiplegic migraine type 1

Katharina Eikermann-Haerter,<sup>1,2</sup> Ergin Dileköz,<sup>1</sup> Chiho Kudo,<sup>1</sup> Sean I. Savitz,<sup>3</sup> Christian Waeber,<sup>1</sup> Michael J. Baum,<sup>4</sup> Michel D. Ferrari,<sup>5</sup> Arn M.J.M. van den Maagdenberg,<sup>5,6</sup> Michael A. Moskowitz,<sup>1</sup> and Cenk Ayata<sup>1,7</sup>

<sup>1</sup>Stroke and Neurovascular Regulation Laboratory, Department of Radiology, Massachusetts General Hospital, Harvard Medical School, Charlestown, Massachusetts, USA. <sup>2</sup>Department of Neurology, University of Duisburg-Essen, Essen, Germany. <sup>3</sup>Department of Neurology, University of Texas Medical School at Houston, Houston, Texas, USA. <sup>4</sup>Department of Biology, Boston University, Boston, Massachusetts, USA. <sup>5</sup>Department of Neurology and <sup>6</sup>Department of Human Genetics, Leiden University Medical Center, Leiden, The Netherlands. <sup>7</sup>Stroke Service and Neuroscience Intensive Care Unit, Department of Neurology, Massachusetts General Hospital, Harvard Medical School, Boston, Massachusetts, USA.

**Familial hemiplegic migraine type 1 (FHM1) is an autosomal dominant subtype of migraine with aura that is associated with hemiparesis. As with other types of migraine, it affects women more frequently than men. FHM1 is caused by mutations in the *CACNA1A* gene, which encodes the  $\alpha_{1A}$  subunit of  $Ca_v2.1$  channels; the R192Q mutation in *CACNA1A* causes a mild form of FHM1, whereas the S218L mutation causes a severe, often lethal phenotype. Spreading depression (SD), a slowly propagating neuronal and glial cell depolarization that leads to depression of neuronal activity, is the most likely cause of migraine aura. Here, we have shown that transgenic mice expressing R192Q or S218L FHM1 mutations have increased SD frequency and propagation speed; enhanced corticostriatal propagation; and, similar to the human FHM1 phenotype, more severe and prolonged post-SD neurological deficits. The susceptibility to SD and neurological deficits is affected by allele dosage and is higher in S218L than R192Q mutants. Further, female S218L and R192Q mutant mice were more susceptible to SD and neurological deficits than males. This sex difference was abrogated by ovariectomy and senescence and was partially restored by estrogen replacement, implicating ovarian hormones in the observed sex differences in humans with FHM1. These findings demonstrate that genetic and hormonal factors modulate susceptibility to SD and neurological deficits in FHM1 mutant mice, providing a potential mechanism for the phenotypic diversity of human migraine and aura.**

## Introduction

Spreading depression (SD) is characterized by an intense depolarization of neuronal and glial membranes that propagates in brain tissue at a rate of approximately 3 mm/min (1, 2). Evoked when local extracellular  $K^+$  concentrations exceed a critical threshold, SD is associated with disruption of membrane ionic gradients, and massive  $K^+$  efflux and glutamate release; both are believed to depolarize adjacent neurons and glia, thereby facilitating its spread. There is growing evidence from animal experiments, suggesting that cortical SD (CSD) is the electrophysiological event underlying migraine aura and a possible trigger of headache mechanisms (3–5). In humans, evidence for a causal role of SD in the aura comes from functional MRI performed during migraine with aura attacks (6, 7).

SD is also implicated in the pathophysiology of familial hemiplegic migraine (FHM), an autosomal dominant subtype of migraine with aura associated with hemiparesis (8). The aura and headache features are otherwise identical to those in the common, multifactorial forms of migraine. This and the fact that the majority of

FHM patients also experience attacks of common migraine with or without aura (9) make FHM a valid model for studying the pathogenesis of common, complex types of migraine.

Thus far, 3 FHM genes have been identified (10). The FHM1 *CACNA1A* gene encodes the pore-forming  $\alpha_{1A}$ -subunit of neuronal, voltage-gated  $Ca_v2.1$  (previously known as P/Q-type) calcium channels (11, 12). Two knock-in FHM1 mouse models, carrying the human pathogenic R192Q or S218L missense mutation, were generated (13, 14). In patients, the R192Q mutation causes pure FHM without other associated neurological features (12), whereas the S218L mutation causes a severe migraine phenotype with excessive and often fatal cerebral edema (15). When expressed in transfected cultured neurons, both mutations shift channel opening toward more negative membrane potentials and delay channel inactivation; the S218L mutation causes more pronounced single-channel gain of function than R192Q (14, 16). As a result, channels open with smaller depolarization and stay open longer, allowing more  $Ca^{2+}$  to enter presynaptic terminals. FHM1 mouse models exhibit a reduced threshold for electrically evoked CSD and increased SD velocity (13, 17).

Gonadal hormones are important modulators of migraine (18) and cortical excitability (19–21). In migraine with aura, the incidence of attacks reportedly increases during periods of high circulating estrogen (18, 22, 23). Higher plasma estrogen concentrations

**Conflict of interest:** The authors have declared that no conflict of interest exists.

**Nonstandard abbreviations used:** CSD, cortical SD; FHM, familial hemiplegic migraine; SD, spreading depression.

**Citation for this article:** *J. Clin. Invest.* 119:99–109 (2009). doi:10.1172/JCI36059.

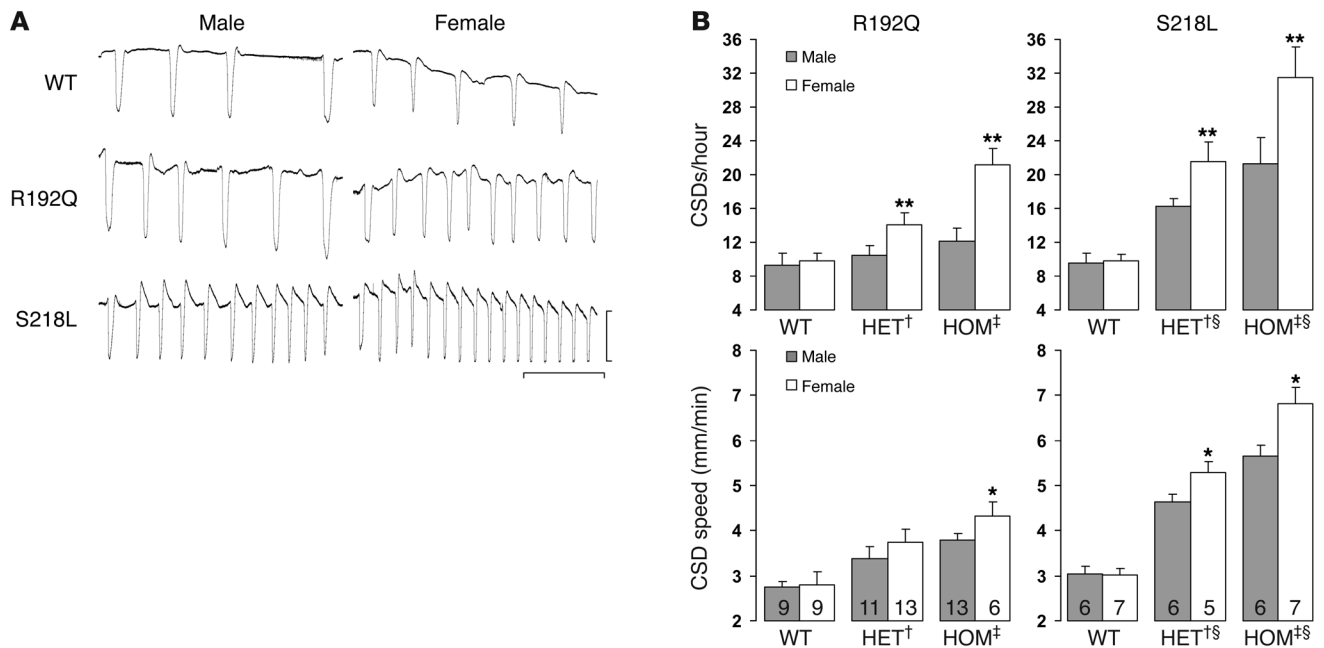


**Figure 1**

Enhanced CSD susceptibility in FHM1 mutant mice. (A) Representative electrophysiological recordings showing increased frequency of slow (DC) potential shifts during repetitive CSDs in male and female homozygous R192Q or S218L mutants compared with WT mice evoked by topical KCl application (300 mM) for 30 minutes. The number of CSDs was substantially higher in FHM1 mutant strains compared with WT controls and in female mutants versus males. Calibration bars: vertical, 20 mV; horizontal, 10 minutes. (B) The impact of R192Q and S218L mutations, allele dosage, and sex on CSD frequency and propagation speed (upper and lower graphs, respectively). Higher CSD frequencies and propagation speeds were found in both FHM1 mutants, with values higher in S218L than in R192Q mutants and an allele dosage relation. CSD frequency was greater and propagation faster in females compared with males in both FHM1 mutant strains. No sex difference was found in WT mice. Covariance analysis revealed that 82% of variation in CSD frequency and 93% of variation in CSD propagation speed were explained by the independent variables mutation, genotype, and sex (see Methods). Numbers of mice per group are shown within the bars. HET, heterozygous; HOM, homozygous. Data are mean ± standard deviation. \*\**P* < 0.001, \**P* < 0.01 versus male in CSD frequency and propagation speed; †*P* < 0.001 versus WT and homozygous mutant; ‡*P* < 0.001 versus WT and heterozygous mutant; §*P* < 0.001 versus corresponding R192Q genotype.

were measured during normal menstrual cycle in migraineurs with aura (24). Whereas the prevalence of migraine is similar in boys and girls before puberty (4%), after puberty it rises to about 3-fold higher in adult females (25%) than in males (8%) (25, 26). A female preponderance is also described for familial (5:2 ratio) and sporadic (4.25:1 ratio) hemiplegic migraine (9, 27, 28).

In this study, we investigated the modulating effect of different allelic mutations, gene dosage, and gonadal hormones on SD susceptibility and subsequent neurological deficits as surrogates for migraine aura in mouse models of FHM1. We found that both FHM1 mutant strains exhibited enhanced SD susceptibility, and SD induced severe and prolonged unilateral motor deficits akin to the human FHM phenotype. Furthermore, both SD susceptibility and severity of neurological deficits were modulated by: (a) the degree of gain of function caused by allelic mutations, (b) allele dosage, and (c) female gonadal hormones. Our data provide a potential mechanism for the severe and prolonged neurological deficits in FHM patients and underscore that genetic and hormonal factors contribute to the phenotypic diversity of human migraine syndromes.

**Results**

*CSD susceptibility in FHM1 mutant mice is modulated by Ca<sub>v</sub>2.1 gain of function, allele dosage, and ovarian hormones.* SD susceptibility was assessed by: (a) counting the number of evoked SDs during continuous topical KCl (300 mM) application and (b) measuring the

propagation speed of SDs between 2 recording electrodes. The values in the different strains were compared. In WT mice, epidural KCl evoked repetitive CSDs (9.5 ± 1.0 SDs/h) with a propagation speed of 2.8 ± 0.2 mm/min. Both the frequency and the propagation speed were increased in the R192Q mutants and even more so in the S218L mutants (Figure 1). Furthermore, heterozygous mice of both FHM1 mutant strains showed SD frequencies and propagation speeds intermediate between those in WT and homozygous mutant mice, indicating an allele dosage effect. The duration or amplitude of SDs after KCl application did not differ among the groups (Table 1). The electrocorticogram did not show seizure activity in mutant mice during these SD recordings under anesthesia.

SD susceptibility (i.e., frequency and propagation speed) was strikingly higher in females than in males of both FHM1 mutant strains but not in WT mice (Figure 1). When tested in R192Q mutant mice, the sex difference was abrogated by ovariectomy, implicating effects of female gonadal hormones in adult brain, rather than a perinatal organizational effect of gonadal hormones or chromosomal sex per se, as modulators of cortical excitability (Figure 2). Consistent with these findings, SD frequencies and propagation speeds were significantly reduced in senescent female R192Q mutant mice after putative cessation of estrous cycling and reduced gonadal hormone production (Figure 2). Chronic estrogen replacement by subcutaneous implantation of pellets containing 0.075 mg 17β-estradiol (3-week release) was associated with a small



**Table 1**  
Electrophysiological measures of CSD and systemic physiological parameters in FHM1 mutant mice

Genotype/sex	Gonadal status	Age (mo)	n	Duration (s)		Amplitude (mV)	MABP	pH	pCO <sub>2</sub>	pO <sub>2</sub>
				1st CSD	All CSDs	All CSDs				
<b>R192Q strain</b>										
WT male	Normal	4.3 ± 0.8	9	42 ± 10	23 ± 11	25 ± 5	81 ± 10	7.36 ± 0.1	38 ± 9	147 ± 19
WT female	Normal	3.7 ± 0.9	9	40 ± 10	16 ± 6	28 ± 3	81 ± 6	7.35 ± 0.03	40 ± 4	133 ± 13
	Ovx	3.7 ± 0.6	10	40 ± 9	18 ± 5	27 ± 3	82 ± 7	7.35 ± 0.03	35 ± 4	139 ± 18
	Ovx + estrogen	3.3 ± 0.0	5	34 ± 6	17 ± 5	30 ± 1	68 ± 6	7.36 ± 0.05	33 ± 4	155 ± 23
	Aged	11.9 ± 1.5	7	26 ± 4	11 ± 3	25 ± 6	83 ± 8	7.38 ± 0.04	30 ± 3	141 ± 22
HET male	Normal	5.2 ± 1.4	11	41 ± 9	19 ± 6	25 ± 7	81 ± 6	7.37 ± 0.06	33 ± 6	133 ± 14
HET female	Normal	4.3 ± 1.3	13	39 ± 11	16 ± 6	24 ± 8	77 ± 6	7.34 ± 0.04	33 ± 6	124 ± 15
HOM male	Normal	4.4 ± 0.8	13	38 ± 10	15 ± 4	24 ± 5	80 ± 6	7.36 ± 0.05	33 ± 6	127 ± 20
HOM female	Normal	3.3 ± 0.4	6	35 ± 7	12 ± 2	30 ± 4	81 ± 4	7.35 ± 0.02	34 ± 2	126 ± 20
	Ovx	4.4 ± 0.9	12	31 ± 6	13 ± 2	28 ± 3	88 ± 4	7.34 ± 0.05	36 ± 9	135 ± 34
	Ovx + estrogen	6.1 ± 0.3	6	30 ± 2	14 ± 2	30 ± 1	79 ± 2	7.38 ± 0.03	31 ± 3	130 ± 22
	Aged	13.0 ± 2.7	7	29 ± 1	13 ± 2	26 ± 1	81 ± 7	7.35 ± 0.04	33 ± 4	153 ± 22
<b>S218L strain</b>										
WT male	Normal	2.7 ± 0.5	6	34 ± 2	14 ± 4	25 ± 2	88 ± 15	7.41 ± 0.03	27 ± 4	148 ± 17
WT female	Normal	2.9 ± 0.7	7	32 ± 7	14 ± 4	25 ± 3	96 ± 7	7.36 ± 0.05	31 ± 4	138 ± 20
HET male	Normal	3.0 ± 0.0	6	29 ± 4	11 ± 2	25 ± 6	93 ± 5	7.41 ± 0.02	29 ± 3	140 ± 9
HET female	Normal	2.6 ± 0.5	5	35 ± 6	11 ± 2	24 ± 2	95 ± 6	7.38 ± 0.01	30 ± 2	144 ± 7
HOM male	Normal	2.7 ± 0.5	6	36 ± 3	12 ± 3	21 ± 5	86 ± 9	7.37 ± 0.03	32 ± 4	126 ± 24
HOM female	Normal	2.6 ± 0.5	7	29 ± 5	10 ± 1	25 ± 4	90 ± 2	7.35 ± 0.03	31 ± 4	134 ± 21

Values are mean ± standard deviation. CSD duration was measured at half amplitude. Because the duration, but not the amplitude, gradually decreased upon repetitive SDs in all groups, both the duration of first CSD and the average of all CSDs are presented. Group differences are not statistically significant (1-way ANOVA). Estrogen: 0.075 mg/pellet 21-day release. Mean arterial blood pressure (MABP) and arterial partial pressure of oxygen (pO<sub>2</sub>) and carbon dioxide (pCO<sub>2</sub>) are expressed in mmHg, averaged over 1-hour recordings. n, number of mice; Ovx, ovariectomized; HET, heterozygous; HOM, homozygous.

increase in SD susceptibility in ovariectomized R192Q mutant, but not in WT, mice (13 ± 1 vs. 16 ± 1 SDs/h in control and estrogen-treated homozygous R192Q mutant, n = 5 and 6, respectively; P < 0.01). A lower dose of estrogen (0.025 mg/pellet) was ineffective in both WT and homozygous R192Q mutant mice (data not shown). Neither gonadectomy nor advanced age influenced SD susceptibility in WT mice using the described protocols (Figure 2). These data suggest that female gonadal hormones modulate SD susceptibility only in mice that have a genetic predisposition.

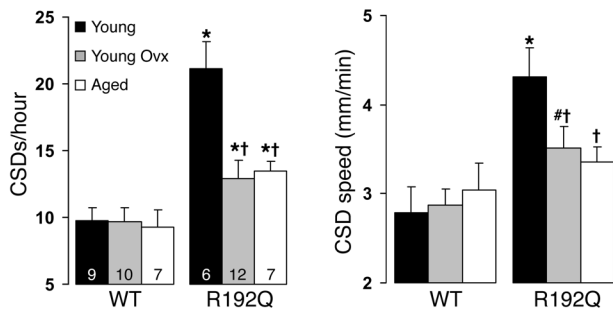
*FHM1 mutant mice develop severe and prolonged motor deficits after SD that are modulated by gene dosage and sex.* Prior to SD induction, both WT and FHM1 mutant strains appeared phenotypically normal and did not exhibit neurological deficits when assessed using the wire grip test and neurological examination protocols. In WT mice, a single SD induced by brief topical application of 300 mM KCl caused only mild deficits that lasted less than 10 minutes in the wire grip test and only a mild and short-lasting hemiparesis that completely recovered before the first neurological assessment at 5 minutes after SD induction (Figure 3A). In contrast, a single SD caused hemiplegia with leaning and circling in both R192Q and S218L mutant mice (Figure 3, Supplemental Figure 1, and Supplemental Videos 1–13; supplemental material available online with this article; doi:10.1172/JCI36059DS1). In the wire grip test, they were initially unable to move along the wire and fell more often than WT mice. S218L mutants were more severely impaired, and unlike R192Q mice, some remained unconscious for up to 10 minutes after a single SD. Homozygous FHM1 mutant mice were impaired more than heterozygotes, indicating an allele dosage relation (Figure 3). Interestingly, FHM1 mutants showed 1 or more transient episodes of neurological deterioration after full or partial recovery during the 60- to 80-minute monitoring period (Supplemental Figure 1E).

All 3 homozygous S218L mutant mice developed generalized seizures 45, 55, and 75 minutes after a single SD. Two of the mice died immediately after the seizure due to respiratory arrest; the third mouse survived the seizure and completely recovered at 80 minutes. Seizures were not observed in heterozygous S218L or homozygous R192Q mutant mice during recovery from SD. The deficits in heterozygous S218L mutant mice in the absence of overt seizure activity suggest that the clinical phenotype was most likely due to SD and not seizure activity.

Compared with a single SD, multiple SDs (9 in 1 hour) caused more severe motor deficits. In WT mice, deficits in the wire grip test were detectable for 30 minutes after the last SD (Figure 3B), whereas multiple SDs caused even more severe deficits in R192Q mutants. Moreover, female R192Q mutant mice developed more severe and longer-lasting deficits than males (Figure 3B).

*Recovery of cortical evoked potentials after SD is not delayed in FHM1 mutant mice.* To test whether prolonged neurological deficits were due to a slower recovery of cortical electrophysiological function, we recorded somatosensory evoked potentials in the whisker barrel cortex after a single SD. Evoked potentials were abolished after SD but reemerged within approximately 2 minutes and completely recovered to pre-SD baseline levels within 10 minutes (Figure 4A). The recovery rate was identical in WT and R192Q or S218L mutant mice (Figure 4, A and B). No seizure activity was observed in these recordings under anesthesia. These data indicated that delayed electrophysiological recovery of cortical synaptic function was not the cause of prolonged and severe unilateral motor deficits after CSD in FHM1 mutant mice.

*Corticostriatal propagation of SD is facilitated in FHM1 mutant mice.* CSD occasionally propagates into subcortical structures in rodent brain (29, 30). We therefore tested whether prolonged post-SD

**Figure 2**

Gonadal hormone-mediated modulation of CSD susceptibility in female FHM1 mutant mice. The impact of ovariectomy and senescence on CSD susceptibility in WT and homozygous R192Q mutant mice. Both ovariectomy (3–4 months of age; gray) and senescence (13 months of age; white) reduced CSD frequency (left panel) and propagation speed (right panel) in homozygous female R192Q to the level of male mutants (see Figure 1B). Ovariectomy ( $n = 5$ ) and aging ( $n = 7$ ) had similar effects in heterozygous female R192Q mice (data not shown). In WT mice, gonadectomy or senescence did not alter CSD susceptibility. Experiments were performed 3 weeks after ovariectomy. Numbers of mice for each group are shown within the bars. Ovx, ovariectomized. Data are mean  $\pm$  standard deviation. \* $P < 0.001$ , # $P < 0.01$  versus WT; † $P < 0.001$  versus naive young female mice of the same genotype.

neurological deficits such as hemiplegia and circling were associated with enhanced subcortical spread into the striatum. In WT mice, CSDs did not reach the striatum (Figure 5; see Methods for experimental conditions). In contrast, CSDs readily propagated into the striatum in FHM1 mutant mice (Figure 5A). Corticostriatal SD propagation was more frequent and arose with shorter latency in S218L compared with R192Q mutant mice ( $P < 0.05$ ), homozygotes compared with heterozygotes of both mutant strains ( $P < 0.01$ ), and female homozygous (but not heterozygous) mutants compared with males ( $P < 0.01$ ; Figure 5B and Table 2). SD did not propagate to thalamus and hippocampus under our experimental conditions ( $n = 7$  heterozygous female and homozygous male S218L mice;  $n = 2$  WT mice; data not shown). Therefore, corticostriatal SD propagation corresponded well to the severity of post-SD neurological deficits and was modulated by: (a) the degree of ion channel dysfunction; (b) allele dosage; and (c) sex. These data implicate corticostriatal SD propagation as a likely explanation for the more severe motor deficits in FHM1 mutant mice.

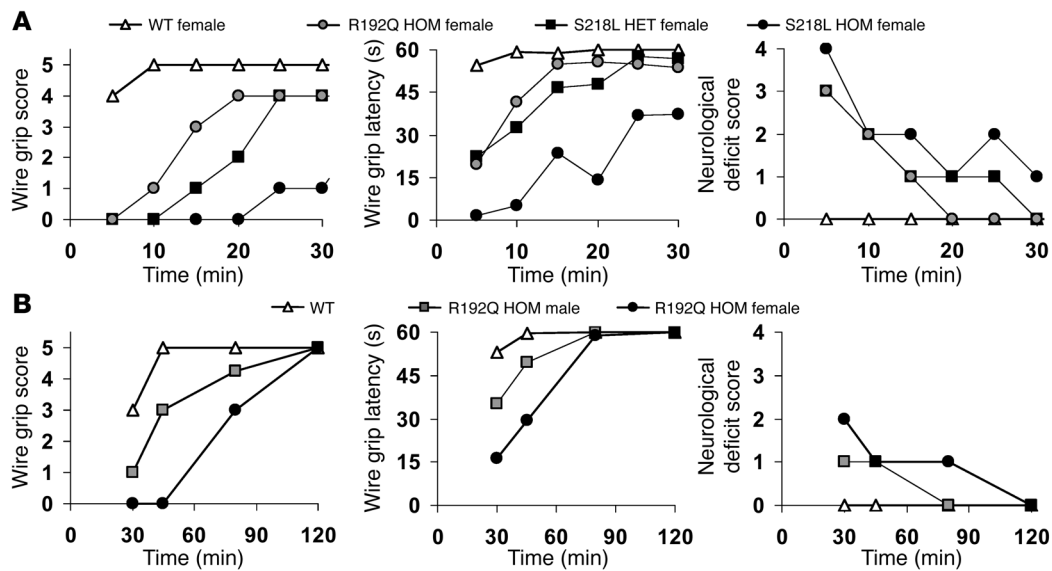
*FHM1 mutant mice develop delayed recurrent SDs after a single KCl-induced SD.* In order to test whether prolonged neurological deficits were caused by recurrent SDs, we recorded from cortex and striatum simultaneously for 60 minutes after one initial SD induced by brief topical KCl application that was followed by extensive saline wash. In all FHM1 knock-in mice, 1 or more recurrent SDs were observed throughout the recording period (range, 1–55 minutes after the initial SD,  $n = 6$  heterozygous female and 2 homozygous male S218L mutants and  $n = 3$  homozygous female R192Q mutants; Supplemental Figure 3). None of the WT mice showed SD recurrence. As suggested by their latency, recurrent SDs appeared to originate from cortex and consistently spread into striatum. In a few instances, there was evidence for cortico-striato-cortical reentrant SDs. In the absence of prior SD induction, we did not observe spontaneous SDs during 60-minute recordings in mutant or WT strains ( $n = 6$ ).

## Discussion

Migraine susceptibility is modulated by genetic, physiological, and environmental factors. Here, we provide experimental evidence showing that genetic ( $Ca_v2.1$  voltage-gated  $Ca^{2+}$  channel mutations) and physiological factors (gonadal hormones) modulating susceptibility to migraine also modulate SD susceptibility. Enhanced SD susceptibility shows a clear relation to the degree of single-channel gain of function caused by S218L and R192Q mutations and is associated with more severe and prolonged neurological deficits after SD, consistent with the clinical phenotypes observed in FHM1 patients. Both enhanced SD susceptibility (i.e., frequency and propagation speed) and neurological deficits are linked to the propensity of corticostriatal SD propagation and are modulated by the interaction of allelic mutations, gene dosage, and gonadal hormones.

The  $Ca_v2.1$  calcium channels are important modulators of SD (31, 32). The first evidence that linked  $Ca_v2.1$  channel mutations to a CSD phenotype was described in tottering and leaner mice. These naturally occurring mouse mutants have loss-of-function mutations in their  $Ca_v2.1$  channels and showed an *increase* in SD threshold (33). In a subsequent study, van den Maagdenberg and colleagues (13) demonstrated a *reduced* threshold for SD induced by electrical stimulation in R192Q FHM1 mutant mice. The increased SD frequency and propagation speed following epidural KCl application in R192Q mutant mice in the present study are in line with these results. Consistent with more negative opening voltages and a greater increase in the single-channel opening probability associated with S218L mutation, SD susceptibility was even higher in this mutant, suggesting incremental modulation of the phenotype by allelic mutations (13, 14, 16). Because excitatory neurotransmitters promote SD via NMDA receptors (34–38), we speculate that FHM1 mutations facilitate the initiation and propagation of SDs by increasing presynaptic  $Ca^{2+}$  influx and subsequent glutamate release. Although augmented neurotransmitter release has been shown at the neuromuscular junctions of R192Q mutant mice (13, 39), this remains to be tested in central synapses.

*Sex hormones.* Our data establish the importance of female gonadal hormones as modulators of genetically driven enhanced SD susceptibility. Ovarian hormones, rather than sex chromosome-related developmental differences in synaptic organization and structure, were implicated in aged female mice and after ovariectomy. These findings may be clinically relevant, since migraine improves at menopause in two-thirds of patients (40). The frequency of migraine attacks decreases after age 50, both in patients with FHM and those with more typical migraine subtypes (9). Estradiol did partially restore SD susceptibility when administered chronically to ovariectomized R192Q mutant mice. Clinically, estrogen reportedly increases cortical excitability in humans during transcranial magnetic stimulation (41), and high doses increase the incidence of aura during hormone replacement therapy (42–44). Moreover, higher levels of estrogen are associated with an increase in seizure frequency in females (45). Experimentally, seizure thresholds are decreased during peak estrogen levels (46), and amygdala kindling is increased (47). Estrogen augments excitatory glutamatergic neurotransmission by upregulating NMDA receptor expression, downregulating glutamate uptake by astrocytes, and increasing the number of dendritic spines, which are densely populated with NMDA receptors (19–21). A large body of evidence suggests that estrogen modulates nociceptive processing as well (48, 49), so that enhanced SD susceptibility is only one mechanism by which estrogen may impact migraine.

**Figure 3**

Prolonged and severe neurological deficits after SD in FHM1 mutant mice. Time course of neurological deficits in WT and FHM1 mutant mice after a single SD (A) or 9 SDs over 1 hour (B), as assessed by wire grip score and latency as well as neurological score. (A) Impact of allelic mutations and allele dosage. In WT mice, deficits were mild and short-lasting in wire grip test and undetectable by neurological scoring (triangles). FHM1 mutants developed severe and prolonged deficits ( $P < 0.01$  versus WT). These deficits were markedly more severe and prolonged in homozygous S218L (black circles) than in homozygous R192Q mutants (gray circles;  $P < 0.01$ ) or heterozygous S218L mutants (squares;  $P < 0.01$  in wire grip test,  $P < 0.05$  in neurological scoring).  $n = 13, 7, 6,$  and  $3$  WT, homozygous R192Q, heterozygous S218L, and homozygous S218L mutant mice, respectively. (B) Sex differences. In WT mice, deficits were mild and completely recovered within 45 minutes after 9 SDs. In contrast, R192Q mutant mice developed severe and prolonged deficits that lasted 80 minutes or more after 9 SDs ( $P < 0.01$  versus WT). Importantly, female mutant mice (circles) were more severely affected than males (squares;  $P < 0.01$ ). Deficits did not differ between WT males and females; therefore, data were pooled (triangles).  $n = 15, 6,$  and  $7$  WT, male R192Q, and female R192Q mutant mice, respectively. Error bars were omitted for clarity but were less than 25% of mean.

Clinical and epidemiological data on hormonal modulation of FHM are sparse. In a population-based study, the female/male ratio was 5:2; males and females did not differ in age of onset or in symptoms of aura and headache (9). In one case report, a 48-year-old woman with hemiplegic migraine ceased to experience any further neurological signs during migraine attacks after ovariectomy (50). Hence, available evidence supports the notion that female gonadal hormones aggravate the hemiplegic migraine phenotype as well.

The lack of gonadal hormone modulation of SD in WT mice we observed argues against a simple additive effect between genetic and hormonal factors and suggests that gonadal hormones modulate SD susceptibility predominantly in brains made susceptible by gene mutations. The precise nature of the interactions between gonadal hormones and mutant  $Ca_v2.1$  channels remains to be determined. It has been shown, however, that estrogen upregulates expression of some voltage-gated  $Ca^{2+}$  channels (e.g., L- and T-type) in hypothalamus and pituitary (51–53). Expression levels of the  $\alpha_{1A}$  subunit of P/Q-type channels show sexual dimorphism in anterior pituitary (higher in females than in males) and fluctuate during estrous cycle, suggesting a direct modulation by female hormones (54). Furthermore,  $Ca_v2.1$  channels undergo extensive alternative splicing that shows sexual dimorphism (55). Therefore, female hormones may enhance the impact of genotype on SD phenotype via increased expression or by favoring alternative splicing patterns that enhance mutant channel activity.

It should be noted that Brennan et al. recently reported that SD thresholds are reduced by approximately 50% in WT female mice

compared with males (56). Using the SD frequency model, we did not detect sex differences in the WT strain, despite 95% power to detect a 25% difference between the means in our model ( $\alpha = 0.05$ ). We also did not detect a threshold difference using direct epidural cortical electrical stimulation (140  $\mu\text{m}$  tip diameter, 200  $\mu\text{m}$  tip separation, 4.3 k $\Omega$  tip resistance) very similar to that used by Brennan et al. (56) (electrical SD threshold,  $413 \pm 168$  [females] vs.  $460 \pm 124$  [males]  $\mu\text{C}$ ,  $n = 11$  and  $8$ , respectively;  $P = 0.7$ ). At present, we do not have an explanation for the discrepant results. Nevertheless, consistent with our data, the propagation speed, SD duration, and number of successful SD inductions did not differ between WT males and females in their study, and the studies agree that gonadal hormones play an important part in modulating SD susceptibility.

**Motor deficits.** Motor deficits (i.e., contralateral hemiplegia with leaning and circling) were significantly more severe and prolonged in FHM1 mutant mice, as compared with the WT strain, lasting 20 minutes or more after induction of a single SD. As can be expected from single-channel kinetics (14), the deficits were more severe in S218L than in R192Q mutant mice, and often experiments were terminated by fatal generalized seizures. Delayed electrophysiological recovery of cortical function did not explain the post-SD deficits (Figure 4). Instead, we believe that the propagation of CSD into the striatum in FHM1 mutants may have been responsible. The frequency of striatal SDs (as well as their propagation speed from cortex to striatum) was greater in the homozygous mutants, in female mutant mice, and in the S218L strain, i.e., the one with the most severe calcium channel dysfunction (14).

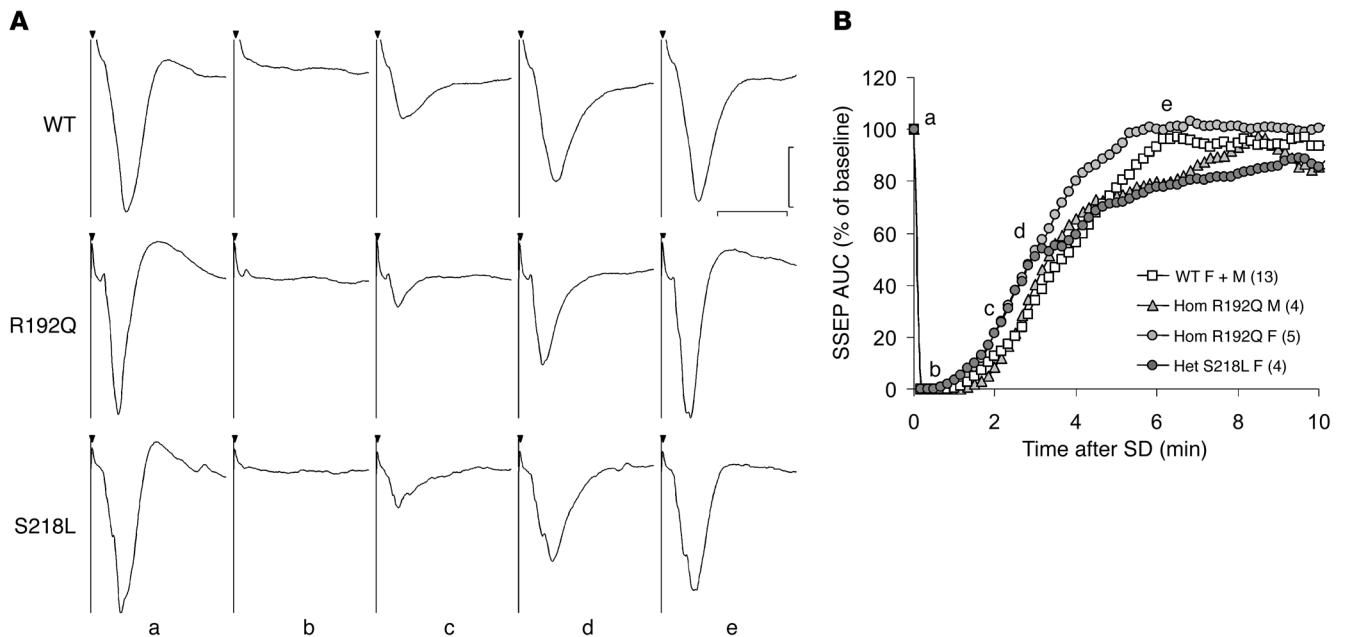


**Figure 4**

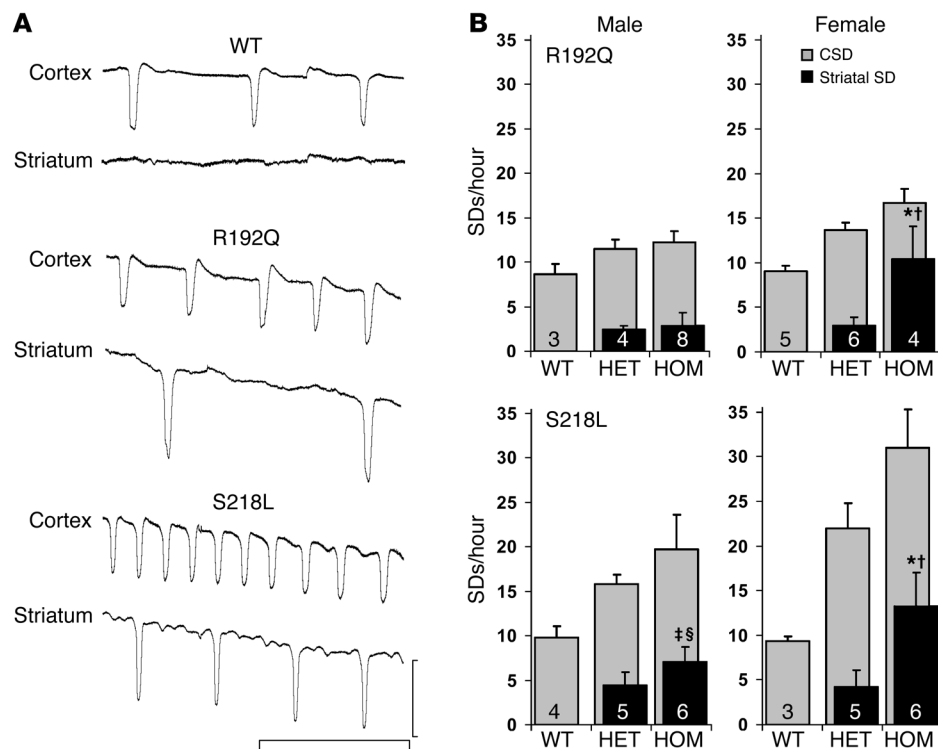
The recovery of whisker pad stimulation–evoked cortical field potentials. **(A)** Representative tracings showing field potentials in a female WT (top), homozygous female R192Q mutant (middle), and heterozygous female S218L mutant mouse (bottom), evoked by electrical stimulation of the whisker pad (black triangles) and recorded from the whisker barrel field using extracellular glass micropipettes (400  $\mu$ m depth, layer IV). Evoked potentials ranging from 2 to 4 mV in amplitude at baseline (column a) were abolished upon arrival of SD at the recording site (column b) and gradually recovered within less than 10 minutes (columns c–e), as shown in the time course graph in **B**. Calibration bars: vertical, 1 mV; horizontal, 20 ms. **(B)** The time course of recovery of somatosensory evoked field potentials (SSEP) after a single SD (time 0). The AUC for each evoked field potential (mV  $\cdot$  ms) was expressed as percent of pre-SD baseline. The rate of recovery of cortical evoked field potentials did not differ among WT and FHM1 mutant mice. Recovery of peak amplitudes also did not differ among groups (data not shown). Numbers of mice are indicated in the graph. Male and female WT mice did not differ; therefore, pooled data are shown. Error bars were omitted for clarity.

Striatal SDs are associated with contralateral circling and hemiparesis (57–59). CSDs did not propagate into the striatum in WT mice, consistent with the absence of severe neurological deficits. CSD spreads into the striatum through the amygdala as SD propagation is impeded in tissues such as white matter with less than a critical density of neurons (1, 29, 30, 60–62). Consistent with this, direct thalamic and hippocampal electrophysiological recordings failed to detect concurrent SD propagation into these structures in either WT or FHM knock-in mouse. In rats, the proportion of CSD propagating into striatum reportedly varied between 4% and 60% in different studies, depending on the strain and the use and type of anesthesia, and subcortical propagation of CSD could be facilitated pharmacologically (e.g., with pyrrolopyrimidine BW 58271) or physiologically (e.g., in undernourished rats) (30, 59, 60). To our knowledge, this has not been studied in mice at this level of detail. Our data suggest that FHM1 mutations facilitate corticostriatal SD propagation. The anesthetic regimen used in our model may explain the complete lack of corticostriatal SD propagation in WT mice (63, 64).

Post-SD neurological deficits were not only more severe in the mutant strains but also lasted longer than in WT mice. Indeed, mutants showed one or more episodes of transient neurological worsening, delaying the neurological recovery after a single KCl-induced SD. Prolonged deficits and episodes of transient worsening were linked to recurrent and possibly reentrant SDs in FHM1 mutants. It should also be noted that SD causes severe and long-lasting tissue hypoperfusion (65) and hypoxia in mice (66).

It remains to be tested whether the hemodynamic and metabolic impact of SD is more severe in FHM1 mice and whether this contributes to the prolonged post-SD neurological deficits.

**Seizures.** Recurrent SDs observed in FHM1 mutants might have directly caused or predisposed to delayed seizures in the S218L knock-in. Homozygous female S218L knock-in mice developed generalized seizures 45–75 minutes after a single SD. Interestingly, the incidence of premature death at a young age (i.e., <20 weeks, both males and females) was higher in mice of both knock-in strains, in some cases linked to apparently spontaneous seizures (our unpublished observations), suggesting that FHM1 mutations predispose to seizures without an experimentally triggered SD. SD may also render the cortex transiently hyperexcitable. For example, SD enhances excitatory postsynaptic field potentials as well as the repetition rate and amplitude of spontaneous rhythmic potentials 20–90 minutes after its induction; it augments long-term potentiation in human neocortical slices (67, 68). SD is followed by hyperexcitability in rat neocortex and spinal cord after transient depression of neuronal activity (69, 70). Last but not least, SD can directly precipitate seizure-like electrocorticogram activity, as first demonstrated by Leão (2). Consistent with our findings, epilepsy is more frequent in FHM patients than in the general population, with seizures occurring either during FHM attacks (71–74) or interictally (75–78). Epilepsy has been reported in many patients carrying FHM1 mutations (10, 71, 79–82). For example, 2 patients harboring the S218L mutation have developed seizures at the onset of severe attacks associated with coma (15, 83).

**Figure 5**

Facilitated corticostriatal SD propagation in FHM1 mutant mice. (A) Representative extracellular DC potential shifts recorded simultaneously from cortex and striatum in female WT and homozygous R192Q and S218L mutant mice. SD was not observed to propagate into the striatum in any of the WT mice. A substantial proportion of CSDs propagated into the striatum in R192Q and to a greater extent in the S218L mutant. Calibration bars: vertical, 20 mV; horizontal, 10 minutes. (B) The frequency of SDs during continuous topical KCl application (300 mM) to the occipital cortex. CSD frequency (gray bars) was substantially higher in S218L and to a lesser extent in R192Q mutant mice than WT. They were higher in females compared with males and homozygous FHM1 mutants compared with heterozygotes (see Figure 1). CSDs readily propagated into striatum (black bars) in both FHM1 mutant strains, but never in the WT. Striatal propagation was more frequent in S218L (lower graphs) compared with R192Q mutants (upper graphs) and in females (right) compared with males (left), with an allele dosage relation (see Table 2 for latencies between cortical and striatal SDs). Covariance analysis revealed that 83% of the variance of striatal SD frequency was explained by the independent variables mutation, genotype, and sex (see Methods).  $n = 3-8$  mice per group as shown within each bar. Data are mean  $\pm$  standard deviation. \* $P < 0.01$  versus male; † $P < 0.001$ , § $P < 0.05$  versus heterozygous mutants; ‡ $P < 0.01$  versus R192Q males.

In summary, data showing enhanced SD susceptibility and prolonged neurological deficits after SD in genetic mouse models of migraine strengthen the link between SD and the migraine aura. Furthermore, they provide mechanistic insight by implicating recurrent SDs and facilitated propagation of SD into subcortical tissues. The modulation of SD susceptibility, neurological deficits, and subcortical propagation by specific FHM1 mutations (i.e., R192Q vs. S218L mutation), genotype (i.e., heterozygous vs. homozygous), and gonadal hormones underscores the complex synergistic interactions between genetic and hormonal factors determining migraine susceptibility.

## Methods

**Experimental groups.** Experimental groups are summarized in Table 1. A total of 337 mice were used in this study. Male and female FHM1 mutant mice, homozygous or heterozygous for R192Q or S218L mutation in the mouse *Cacna1a* gene (encoding the  $\alpha_{1A}$  pore-forming subunit of  $Ca_v2.1$

channels), were compared with WT littermates. In addition, R192Q mutants were backcrossed onto C57BL/6J mice (Charles River Laboratories) for more than 8 generations. None of the measured endpoints differed between WT littermates of R192Q mutant and C57BL/6J control mice (data not shown). Therefore, data from WT littermates of R192Q mutants and C57BL/6J control mice were pooled for the analysis. The S218L mutants were compared with their littermates only.

**Preparation of targeting construct and generation of FHM1 mutant mice.** Transgenic knock-in  $Ca_v2.1-\alpha_{1A}$  migraine mouse models were generated by a gene targeting approach in which the endogenous *Cacna1a* gene was modified. In the R192Q mice (13), we modified the CGG triplet (arginine) of codon 192 to CAG (glutamine) using in vitro mutagenesis to introduce the human FHM1 mutation R192Q (12). The targeting vector that was used for generating the S218L mice contained the mutant TTA (leucine) instead of the original TCA (serine) triplet of codon 218; thus creating the S218L mutation that had previously been found in patients (15). This targeting vector also contained a PGK-driven neomycin-resistance cassette that was flanked by *loxP* sites in the endogenous *HindIII* site that is located 537 nucleotides upstream of exon 5. Chimeras were obtained by injecting correctly targeted E14 ES cells into C57BL/6J blastocysts according to standard procedures in order to generate a transgenic line of mice. In mice that were used for the experiments, the cassette was deleted by crossing these transgenic mice with mice of the EIIA-Cre deleter strain (84), which express Cre recombinase driven by the EIIA early promoter.

For both the R192Q and S218L mice, heterozygous mice (>96% C57BL/6J background) were subsequently interbred to provide litters containing all 3 possible genotypes that were used for the experiments. Litters were genotyped after weaning by PCRs specific for the respective transgenic line, essentially as described previously (13). All experiments were carried out with the investigator blinded for genotype, and confirmatory genotyping was done after the experiment. All animal experiments were approved by the Massachusetts General Hospital Subcommittee on Research Animal Care and performed in accordance with the NIH *Guide for the care and use of laboratory animals* (NIH publication no. 85-23. Revised 1985).

**General surgical and electrophysiological procedures.** Mice were housed under diurnal lighting conditions and allowed food and tap water ad libitum. To assess SD susceptibility under full systemic physiological monitoring, femoral artery was catheterized for blood sampling and measurement of mean arterial pressure and trachea intubated for mechanical ventilation (SAR-830; CWE), under isoflurane anesthesia (2.5% induction, 1% maintenance, in 70%  $N_2O/30\% O_2$ ). Arterial blood gases and pH were measured



**Table 2**  
Corticostriatal propagation latency of SD

Strain	Genotype	Male	Female
R192Q	HET	3.7 ± 0.3	4.0 ± 0.6
	HOM	3.5 ± 0.5	1.5 ± 0.2 <sup>A,B</sup>
S218L	HET	3.3 ± 0.8	3.6 ± 0.5
	HOM	2.0 ± 0.6 <sup>A,C</sup>	1.5 ± 0.3 <sup>A</sup>

Values are mean ± standard deviation, expressed in minutes. <sup>A</sup>*P* < 0.01 versus heterozygote; <sup>B</sup>*P* < 0.01 vs. male; <sup>C</sup>*P* < 0.01 versus R192Q. See Figure 5 for the number of mice in each group.

once every 20 minutes during each experiment in 25 µl samples (Corning 178 blood gas/pH analyzer; Ciba Corning Diagnostic Corp.) and maintained within normal limits by adjusting ventilation parameters (Table 1). Mice were then placed in a stereotaxic frame (David Kopf Instruments), and 3 burr holes were drilled under saline cooling at the following coordinates on both sides (mm from bregma): 3.5 mm posterior, 2 mm lateral (2 mm diameter for KCl application onto occipital cortex); 1.5 mm posterior, 2 mm lateral (1 mm diameter, recording site 1); 0.5 mm anterior, 2 mm lateral (1 mm diameter, recording site 2). The dura was kept intact to minimize trauma. Two glass capillary microelectrodes were placed to record extracellular steady (DC) potential and electrocorticogram (ECoG) at a depth of 300 µm. For striatal recordings, the electrode at recording site 2 was lowered to a depth of 3 mm into the striatum. A third electrode was simultaneously inserted at 2 mm posterior, 1.2 mm lateral from bregma, at depths of 3 and 1.2 mm from the pial surface for thalamic and hippocampal recordings, respectively. Recording sites were later confirmed by tracking the electrode placement (Supplemental Figure 2). An Ag/AgCl reference electrode was placed subcutaneously in the neck. Recording sites were covered with mineral oil after electrode placement to prevent cortical drying. After surgical preparation, the occipital cortex was allowed to recover for 20 minutes under saline irrigation. A cotton ball (2 mm diameter) soaked with 300 mM KCl was placed on the dura and replaced every 15 minutes to maintain steady KCl concentration during stimulation. In order to test whether occipital epidural KCl application causes SD in the striatum via direct diffusion, in a subgroup of FHM1 mutant mice we evoked SD by pinprick on the occipital cortex and observed reproducible propagation of SD into striatum with the same latency as after topical KCl application (*n* = 3 female R192Q mutant mice; data not shown). All data were continuously recorded using a data acquisition system for off-line analysis (PowerLab; ADInstruments).

The frequency of SDs evoked by topical KCl application and their propagation speed were determined as previously described with minor modifications (4). KCl-evoked CSDs were detected based on the characteristic slow DC potential shift and ECoG suppression. The frequency of evoked CSDs was determined over 30 minutes on each hemisphere. CSD frequencies obtained from the right and left hemispheres did not statistically differ in any experimental group and were averaged to calculate the CSD frequency in each mouse. Propagation speed was calculated from the distance between the 2 recording electrodes divided by the latency between the first CSDs recorded at these sites. The DC shift amplitude and duration at half-maximal amplitude were averaged for all CSDs in each experiment.

Epidural application of NaCl (300 mM) did not trigger SD or cause neurological deficits in sham-operated knock-in controls (*n* = 2 homozygous female R192Q mutant mice; data not shown). In subgroups of WT and FHM1 mutant mice, histopathological assessment of the KCl application site after the experimental recordings did not reveal any evidence of cortical injury in H&E-stained frozen sections (data not shown).

**Ovariectomy and estrogen replacement.** The impact of diminished gonadal hormone production on SD susceptibility was studied using ovariectomized (3–4 months old) or senescent (13 months old, after cessation of estrous cycle) homozygous R192Q mutant mice. Because the sex effect on SD phenotype appeared in both heterozygous and homozygous mutants (Figure 1), further experiments exploring post-SD neurological deficits (see below) were performed on homozygous mutants only. Ovaries were exteriorized, ligated, and removed via bilateral dorsal approach in young adult mice (3–4 months old) under isoflurane anesthesia. In addition, subgroups of ovariectomized mice were chronically treated with estrogen via subcutaneous implantation (dorsal scapular) of 21-day slow-release pellets (Innovative Research of America) containing 17β-estradiol 3-benzoate to achieve constant plasma estrogen levels corresponding to the proestrus stage of cycle (0.025 mg/pellet) or higher-than-normal estradiol concentration (0.075 mg/pellet) (85–90). SD susceptibility was tested 3 weeks after ovariectomy with or without estrogen replacement (i.e., empty pellet implantation). The C57BL/6J background of FHM1 mutant mice has a gonadal hormone profile of aging very similar to that observed in menopausal women: prolonged cycles with delayed preovulatory rise of estrogen progress to acyclicity, lower estrogen levels, and hypergonadotrophic hypogonadism (91, 92); decreased nuclear estrogen receptors and a nuclear translocation defect of estrogen-receptor complex have also been described as in humans (93–95).

**Neurological testing.** In order to minimize the confounding effect of invasive surgical procedures on neurological testing, arterial and tracheal catheterizations were not performed, and freely breathing mice were anesthetized via a face mask during the SD induction procedure. Neurological deficits were assessed either after 1 SD or after 9 SDs induced over 1 hour. In the 1-SD group, mice were briefly anesthetized, and KCl (300 mM) was topically applied (typically for less than 1 minute) on the parietooccipital cortex until an SD was recorded in the frontal cortex as described above, followed by extensive saline wash of cortical surface. In the 9-SD group, KCl (300 mM) was briefly applied in the same manner approximately every 7.5 minutes, and SD induction confirmed at the frontal recording site. Motor deficits were assessed at predefined time points after induction of the last SD in a blinded fashion. Mice fully awakened from anesthesia usually within 3 minutes in the 1-SD group; therefore, neurological assessments were started 5 minutes after SD induction and carried out every 5 minutes until full reversal of deficits. Because full awakening was delayed in the 9-SD group for up to 15–20 minutes in all groups, first neurological assessment was carried out 30 minutes after the last SD and then repeated at 45, 80, and 120 minutes. The severity of deficits and high mortality after a single SD in S218L mutant mice precluded testing of the 9-SD paradigm in this strain. There was no difference among WT and FHM1 mutant strains in the time required for full recovery of neurological function after 10 minutes of isoflurane anesthesia (data not shown).

We relied exclusively upon motor performance, since preliminary studies of sensory deficits and neglect (e.g., corner test) did not reliably detect deficits in this model (data not shown). Motor deficits were assessed using 2 independent tests. The 5-point neurological scale is most commonly used to quantify unilateral motor deficits after stroke. The deficits are scored as: 0 (no neurological deficit: normal), 1 (mild neurological deficit: failure to extend forepaw fully), 2 (moderate neurological deficit: circling), 3 (severe neurological deficit: falling to one side), 4 (very severe neurological deficit: no spontaneous walking, depressed level of consciousness), as previously described (96). The wire grip test is used to assess coordination and fine movement of the digits based on the ability of the mouse to remain on the wire and successfully climb down the pole and scored as: 0, unable to remain on wire more than 30 seconds; 1, holds on wire more than 30 seconds, but not with both sets of paws on wire; 2, holds on to the wire with all paws but not the tail; 3, uses the tail along with all paws but does not move on wire; 4,



moves along the wire on all 4 paws plus tail; 5, moves along the wire on all 4 paws plus tail and ambulates down one of the posts used to support the wire. Besides the wire grip score, we also recorded the latency to fall off the wire; if the mouse stayed on the wire for more than 60 seconds, or climbed down the pole successfully, it was scored as 60 seconds (97).

**Somatosensory evoked potentials.** Two cranial windows (1 mm diameter) were drilled under saline cooling over the right whisker barrel cortex (posterior 1.3 mm, lateral 3.7 mm from bregma) and occipital cortex (posterior 4 mm, lateral 2 mm from bregma). The dura was kept intact. A glass micropipette electrode filled with 150 mM NaCl was inserted to a depth of 400  $\mu$ m. Somatosensory evoked potentials as well as the extracellular steady (DC) potential were recorded using a differential amplifier (EX-1; Dagan Corp.) and stored using a data acquisition system for off-line analysis (PowerLab 200; ADInstruments). An Ag/AgCl reference electrode was also placed subcutaneously in the neck, and the cortex was covered with a thin layer of mineral oil to prevent drying. Somatosensory potentials in the whisker barrel cortex were evoked by electrical stimulation of the entire whisker pad (single square pulse, 0.2 ms duration, 700  $\mu$ A, 0.1 Hz; S48, Grass Technologies; and A395 Linear Stimulus Isolator/Constant Current Unit, WPI) via 2 needle electrodes placed in the contralateral whisker pad (5 mm electrode separation). In preliminary experiments, we determined that nitrous oxide in inhalation gas potentially suppressed somatosensory evoked potentials. Therefore, in these experiments, we replaced nitrous oxide with nitrogen.

Whisker pad stimulation typically evoked a monophasic negative field potential at this recording depth (Figure 4). After acquiring 50 such evoked potentials at baseline, a CSD was triggered using brief occipital epidural KCl application and confirmed by the characteristic DC potential shift at the recording site in whisker barrel cortex. In order to avoid multiple CSDs, the KCl application site was immediately washed with saline upon detection of the SD at the recording site. Experiments with multiple SDs were excluded from analysis. Both the amplitude of negative peak and the area under the field potential curve were measured before, during, and after SD and expressed as percent of baseline.

**Statistics.** Data were analyzed using SPSS software package (version 11.0). The impact of independent variables allelic mutations (R192Q vs. S218L), allele dosage (WT, heterozygous, homozygous), and sex (male vs. female) on the dependent variables cortical and striatal SD frequency and propagation speed were tested using 3-way ANOVA (Figures 1 and 5). The impact of independent variables R192Q mutation (WT vs. R192Q) and gonadal

status (normal, ovariectomized, and senescent) on the dependent variables CSD frequency and propagation speed were tested using 2-way ANOVA (Figure 2). The time course of neurological deficits and recovery of somatosensory evoked potentials after SD were tested among experimental groups using 2-way ANOVA for repeated measures (Figures 3 and 4). Electrophysiological measures of CSD (Table 1), systemic physiological data (Table 1), and the impact of estrogen replacement in ovariectomized FHM1 mutant mice (see Results) were compared among experimental groups using 1-way ANOVA. Corticostriatal propagation latencies were compared using 3-way ANOVA (Table 2). In addition, using pooled data from all mice and a general linear model of covariance analysis (ANACOVA), we tested for an effect of the independent variables mutation, genotype, and sex (fixed factors) on the dependent variables cortical and striatal SD frequency and propagation speed. Data are presented as mean  $\pm$  standard deviation.  $P < 0.05$  was considered statistically significant.

### Acknowledgments

This work was supported by the Deutsche Forschungsgemeinschaft (Ha5085/1-1 to K. Eikermann-Haerter), National Institute of Neurological Disorders and Stroke (1R01NS061505 to C. Ayata; 2P01NS35611 to M.A. Moskowitz), Netherlands Organization for Scientific Research (903-52-291 and Vici 918.56.602 to M.D. Ferrari), EU "EUROHEAD" grant (LSHM-CT-2004-504837 to M.D. Ferrari, A.M.J.M. van den Maagdenberg), and the Centre for Medical Systems Biology (CMSB) in the framework of the Netherlands Genomics Initiative (NGI). We would like to thank Elkan Halpern and Tobias Kurth for statistical guidance, Lynda Banzi for assistance with videos, Mike Whalen and Zerong You for assistance with neurological deficit assessment, and Jianhua Qiu for histological imaging.

Received for publication April 28, 2008, and accepted in revised form October 8, 2008.

Address correspondence to: Cenik Ayata, Stroke and Neurovascular Regulation Laboratory, Massachusetts General Hospital, 149 13th Street, Room 6403, Charlestown, Massachusetts 02129, USA. Phone: (617) 726-8021; Fax: (617) 726-2547; E-mail: cayata@partners.org.

- Somjen, G.G. 2001. Mechanisms of spreading depression and hypoxic spreading depression-like depolarization. *Physiol. Rev.* **81**:1065–1096.
- Leao, A.A.P. 1944. Spreading depression of activity in cerebral cortex. *J. Neurophysiol.* **7**:359–390.
- Bolay, H., et al. 2002. Intrinsic brain activity triggers trigeminal meningeal afferents in a migraine model. *Nat. Med.* **8**:136–142.
- Ayata, C., Jin, H., Kudo, C., Dalkara, T., and Moskowitz, M.A. 2006. Suppression of cortical spreading depression in migraine prophylaxis. *Ann. Neurol.* **59**:652–661.
- Lauritzen, M. 1994. Pathophysiology of the migraine aura: the spreading depression theory. *Brain.* **117**:199–210.
- Hadjikhani, N., et al. 2001. Mechanisms of migraine aura revealed by functional MRI in human visual cortex. *Proc. Natl. Acad. Sci. U. S. A.* **98**:4687–4692.
- Cao, Y., Welch, K.M., Aurora, S., and Vikingstad, E.M. 1999. Functional MRI-BOLD of visually triggered headache in patients with migraine. *Arch. Neurol.* **56**:548–554.
- International Headache Society. 2004. The International Classification of Headache Disorders: 2nd edition. *Cephalalgia.* **24**(Suppl. 1):9–160.
- Thomsen, L.L., et al. 2002. A population-based study of familial hemiplegic migraine suggests revised diagnostic criteria. *Brain.* **125**:1379–1391.
- van den Maagdenberg, A.M., Haan, J., Terwindt, G.M., and Ferrari, M.D. 2007. Migraine: gene mutations and functional consequences. *Curr. Opin. Neurol.* **20**:299–305.
- Pietrobon, D. 2005. Migraine: new molecular mechanisms. *Neuroscientist.* **11**:373–386.
- Ophoff, R.A., et al. 1996. Familial hemiplegic migraine and episodic ataxia type-2 are caused by mutations in the Ca<sup>2+</sup> channel gene CACNL1A4. *Cell.* **87**:543–552.
- van den Maagdenberg, A.M., et al. 2004. A CACNA1a knockin migraine mouse model with increased susceptibility to cortical spreading depression. *Neuron.* **41**:701–710.
- Tottene, A., et al. 2005. Specific kinetic alterations of human CaV2.1 calcium channels produced by mutation S218L causing familial hemiplegic migraine and delayed cerebral edema and coma after minor head trauma. *J. Biol. Chem.* **280**:17678–17686.
- Kors, E.E., et al. 2001. Delayed cerebral edema and fatal coma after minor head trauma: role of the CACNA1A calcium channel subunit gene and relationship with familial hemiplegic migraine. *Ann. Neurol.* **49**:753–760.
- Tottene, A., et al. 2002. Familial hemiplegic migraine mutations increase Ca<sup>2+</sup> influx through single human CaV2.1 channels and decrease maximal CaV2.1 current density in neurons. *Proc. Natl. Acad. Sci. U. S. A.* **99**:13284–13289.
- Pietrobon, D. 2007. Familial hemiplegic migraine. *Neurotherapeutics.* **4**:274–284.
- MacGregor, E.A. 2004. Oestrogen and attacks of migraine with and without aura. *Lancet Neurol.* **3**:354–361.
- Smith, S.S. 1989. Estrogen administration increases neuronal responses to excitatory amino acids as a long-term effect. *Brain Res.* **503**:354–357.
- Sato, K., Matsuki, N., Ohno, Y., and Nakazawa, K. 2003. Estrogens inhibit l-glutamate uptake activity of astrocytes via membrane estrogen receptor alpha. *J. Neurochem.* **86**:1498–1505.
- Woolley, C.S., Weiland, N.G., McEwen, B.S., and Schwartzkroin, P.A. 1997. Estradiol increases the sensitivity of hippocampal CA1 pyramidal cells to NMDA receptor-mediated synaptic input: correlation with dendritic spine density. *J. Neurosci.* **17**:1848–1859.
- Ertresvag, J.M., Zwart, J.A., Helde, G., Johnsen, H.J., and Bovim, G. 2005. Headache and transient focal neurological symptoms during pregnancy, a pro-



- spective cohort. *Acta Neurol. Scand.* **111**:233–237.
23. Granello, F., et al. 1993. Migraine without aura and reproductive life events: a clinical epidemiological study in 1300 women. *Headache.* **33**:385–389.
  24. Nagel-Leiby, S., Welch, K.M., Grunfeld, S., and D'Andrea, G. 1990. Ovarian steroid levels in migraine with and without aura. *Cephalalgia.* **10**:147–152.
  25. Rasmussen, B.K., Jensen, R., Schroll, M., and Olesen, J. 1991. Epidemiology of headache in a general population — a prevalence study. *J. Clin. Epidemiol.* **44**:1147–1157.
  26. Bille, B.S. 1962. Migraine in school children. A study of the incidence and short-term prognosis, and a clinical, psychological and electroencephalographic comparison between children with migraine and matched controls. *Acta Paediatr. Suppl.* **136**:1–151.
  27. Eriksen, M.K., Thomsen, L.L., and Olesen, J. 2006. Implications of clinical subtypes of migraine with aura. *Headache.* **46**:286–297.
  28. Thomsen, L.L., et al. 2007. The genetic spectrum of a population-based sample of familial hemiplegic migraine. *Brain.* **130**:346–356.
  29. Fífkova, E., and Bures, J. 1964. Spreading depression in the mammalian striatum. *Arch. Int. Physiol. Biochim.* **72**:171–179.
  30. Vinogradova, L.V., Koroleva, V.I., and Bures, J. 1991. Re-entry waves of Leao's spreading depression between neocortex and caudate nucleus. *Brain Res.* **538**:161–164.
  31. Kunkler, P.E., and Kraig, R.P. 2004. P/Q Ca<sup>2+</sup> channel blockade stops spreading depression and related pyramidal neuronal Ca<sup>2+</sup> rise in hippocampal organ culture. *Hippocampus.* **14**:356–367.
  32. Richter, F., Ebersberger, A., and Schaible, H.G. 2002. Blockade of voltage-gated calcium channels in rat inhibits repetitive cortical spreading depression. *Neurosci. Lett.* **334**:123–126.
  33. Ayata, C., Shimizu-Sasamata, M., Lo, E.H., Noebels, J.L., and Moskowitz, M.A. 2000. Impaired neurotransmitter release and elevated threshold for cortical spreading depression in mice with mutations in the alpha1A subunit of P/Q type calcium channels. *Neuroscience.* **95**:639–645.
  34. Marrannes, R., Willems, R., De Prins, E., and Wauquier, A. 1988. Evidence for a role of the N-methyl-D-aspartate (NMDA) receptor in cortical spreading depression in the rat. *Brain Res.* **457**:226–240.
  35. Amemori, T., and Bures, J. 1990. Ketamine blockade of spreading depression: rapid development of tolerance. *Brain Res.* **519**:351–354.
  36. Jing, J., Aitken, P.G., and Somjen, G.G. 1991. Lasting neuron depression induced by high potassium and its prevention by low calcium and NMDA receptor blockade. *Brain Res.* **557**:177–183.
  37. Nelligard, B., and Wieloch, T. 1992. NMDA-receptor blockers but not NBQX, an AMPA-receptor antagonist, inhibit spreading depression in the rat brain. *Acta Physiol. Scand.* **146**:497–503.
  38. McLachlan, R.S. 1992. Suppression of spreading depression of Leao in neocortex by an N-methyl-D-aspartate receptor antagonist. *Can. J. Neurol. Sci.* **19**:487–491.
  39. Kaja, S., et al. 2005. Gene dosage-dependent transmitter release changes at neuromuscular synapses of CACNA1A R192Q knockin mice are non-progressive and do not lead to morphological changes or muscle weakness. *Neuroscience.* **135**:81–95.
  40. Fettes, I. 1999. Migraine in the menopause. *Neurology.* **53**:S29–S33.
  41. Smith, M.J., Adams, L.F., Schmidt, P.J., Rubinow, D.R., and Wassermann, E.M. 2002. Effects of ovarian hormones on human cortical excitability. *Ann. Neurol.* **51**:599–603.
  42. Aegidius, K.L., Zwart, J.A., Hagen, K., Schei, B., and Stovner, L.J. 2007. Hormone replacement therapy and headache prevalence in postmenopausal women. The Head-HUNT study. *Eur. J. Neurol.* **14**:73–78.
  43. MacGregor, A. 1999. Estrogen replacement and migraine aura. *Headache.* **39**:674–678.
  44. Kaiser, H.J., and Meienberg, O. 1993. Deterioration or onset of migraine under oestrogen replacement therapy in the menopause. *J. Neurol.* **240**:195–196.
  45. Klein, P., and Herzog, A.G. 1998. Hormonal effects on epilepsy in women. *Epilepsia.* **39**(Suppl. 8):S9–S16.
  46. Woolley, D.E., and Timiras, P.S. 1962. Estrous and circadian periodicity and electroshock convulsions in rats. *Am. J. Physiol.* **202**:379–382.
  47. Edwards, H.E., Burnham, W.M., Mendonca, A., Bowlby, D.A., and MacLusky, N.J. 1999. Steroid hormones affect limbic afterdischarge thresholds and kindling rates in adult female rats. *Brain Res.* **838**:136–150.
  48. Okamoto, K., Hirata, H., Takeshita, S., and Bereiter, D.A. 2003. Response properties of TMJ units in superficial laminae at the spinomedullary junction of female rats vary over the estrous cycle. *J. Neurophysiol.* **89**:1467–1477.
  49. Bereiter, D.A., Stanford, L.R., and Barker, D.J. 1980. Hormone-induced enlargement of receptive fields in trigeminal mechanoreceptive neurons. II. Possible mechanisms. *Brain Res.* **184**:411–423.
  50. Sood, S.V. 1971. Hemiplegic migraine associated with menstruation. *J. Obstet. Gynaecol. Br. Commonw.* **78**:762–763.
  51. Qiu, J., et al. 2006. Estrogen upregulates T-type calcium channels in the hypothalamus and pituitary. *J. Neurosci.* **26**:11072–11082.
  52. Sedej, S., Tsujimoto, T., Zorec, R., and Rupnik, M. 2004. Voltage-activated Ca(2+) channels and their role in the endocrine function of the pituitary gland in newborn and adult mice. *J. Physiol.* **555**:769–782.
  53. Ritchie, A.K. 1993. Estrogen increases low voltage-activated calcium current density in GH3 anterior pituitary cells. *Endocrinology.* **132**:1621–1629.
  54. Fiordeliso, T., Jimenez, N., Baba, S., Shiba, K., and Hernandez-Cruz, A. 2007. Immunoreactivity to neurofilaments in the rodent anterior pituitary is associated with the expression of alpha 1A protein subunits of voltage-gated Ca<sup>2+</sup> channels. *J. Neuroendocrinol.* **19**:870–881.
  55. Chang, S.Y., et al. 2007. Age and gender-dependent alternative splicing of P/Q-type calcium channel EF-hand. *Neuroscience.* **145**:1026–1036.
  56. Brennan, K.C., Romero Reyes, M., Lopez Valdes, H.E., Arnold, A.P., and Charles, A.C. 2007. Reduced threshold for cortical spreading depression in female mice. *Ann. Neurol.* **61**:603–606.
  57. Weiss, T., and Fífkova, E. 1963. The effect of neocortical and caudate spreading depression on "circling movements" induced from the caudate nucleus. *Physiol. Bohemoslov.* **12**:332–338.
  58. Trachtenberg, M.C., Hull, C.D., and Buchwald, N.A. 1970. Electrophysiological concomitants of spreading depression in caudate and thalamic nuclei of the cat. *Brain Res.* **20**:219–231.
  59. Jakobartl, L., and Huston, J.P. 1977. Circling and consumatory behavior induced by striatal and neocortical spreading depression. *Physiol. Behav.* **19**:673–677.
  60. DeLuca, B., Shibata, M., Brozek, G., and Bures, J. 1975. Facilitation of Leao's spreading depression by a pyrrolopyrimidine derivative. *Neuropharmacology.* **14**:537–545.
  61. Krivanek, J., and Fífkova, E. 1965. The value of ultramicro-analysis of lactic acid in tracing the penetration of Leao's cortical spreading depression to subcortical areas. *J. Neurol. Sci.* **2**:385–392.
  62. Fífkova, E., and Syka, J. 1964. Relationships between cortical and striatal spreading depression in rat. *Exp. Neurol.* **9**:355–366.
  63. Piper, R.D., and Lambert, G.A. 1996. Inhalational anesthetics inhibit spreading depression: relevance to migraine. *Cephalalgia.* **16**:87–92.
  64. Kitahara, Y., Taga, K., Abe, H., and Shimoji, K. 2001. The effects of anesthetics on cortical spreading depression elicitation and c-fos expression in rats. *J. Neurosurg. Anesthesiol.* **13**:26–32.
  65. Ayata, C., et al. 2004. Pronounced hypoperfusion during spreading depression in mouse cortex. *J. Cereb. Blood Flow Metab.* **24**:1172–1182.
  66. Takano, T., et al. 2007. Cortical spreading depression causes and coincides with tissue hypoxia. *Nat. Neurosci.* **10**:754–762.
  67. Berger, M., Speckmann, E.J., Pape, H.C., and Gorji, A. 2008. Spreading depression enhances human neocortical excitability in vitro. *Cephalalgia.* **28**:558–562.
  68. Footitt, D.R., and Newberry, N.R. 1998. Cortical spreading depression induces an LTP-like effect in rat neocortex in vitro. *Brain Res.* **781**:339–342.
  69. Gorji, A., and Speckmann, E.J. 2004. Spreading depression enhances the spontaneous epileptiform activity in human neocortical tissues. *Eur. J. Neurosci.* **19**:3371–3374.
  70. Gorji, A., Zahn, P.K., Pogatzki, E.M., and Speckmann, E.J. 2004. Spinal and cortical spreading depression enhance spinal cord activity. *Neurobiol. Dis.* **15**:70–79.
  71. Ducros, A., et al. 2001. The clinical spectrum of familial hemiplegic migraine associated with mutations in a neuronal calcium channel. *N. Engl. J. Med.* **345**:17–24.
  72. Ducros, A., et al. 1997. Mapping of a second locus for familial hemiplegic migraine to 1q21-q23 and evidence of further heterogeneity. *Ann. Neurol.* **42**:885–890.
  73. Echenne, B., et al. 1999. Recurrent episodes of coma: an unusual phenotype of familial hemiplegic migraine with linkage to chromosome 1. *Neuropediatrics.* **30**:214–217.
  74. Kramer, U., Lerman-Sagi, T., Margalith, D., and Harel, S. 1997. A family with hemiplegic migraine and focal seizures. *Eur. J. Paediatr. Neurol.* **1**:35–38.
  75. Cevoli, S., et al. 2002. Familial hemiplegic migraine: clinical features and probable linkage to chromosome 1 in an Italian family. *Neurol. Sci.* **23**:7–10.
  76. Jurkat-Rott, K., et al. 2004. Variability of familial hemiplegic migraine with novel A1A2 Na<sup>+</sup>/K<sup>+</sup>-ATPase variants. *Neurology.* **62**:1857–1861.
  77. Terwindt, G.M., et al. 1997. Partial cosegregation of familial hemiplegic migraine and a benign familial infantile epileptic syndrome. *Epilepsia.* **38**:915–921.
  78. Deprez, L., et al. 2008. Epilepsy as part of the phenotype associated with ATP1A2 mutations. *Epilepsia.* **49**:500–508.
  79. Jouvenceau, A., et al. 2001. Human epilepsy associated with dysfunction of the brain P/Q-type calcium channel. *Lancet.* **358**:801–807.
  80. Beauvais, K., et al. 2004. New CACNA1A gene mutation in a case of familial hemiplegic migraine with status epilepticus. *Eur. Neurol.* **52**:58–61.
  81. Vahedi, K., et al. 2000. CACNA1A gene de novo mutation causing hemiplegic migraine, coma, and cerebellar atrophy. *Neurology.* **55**:1040–1042.
  82. Kors, E.E., et al. 2003. Expanding the phenotypic spectrum of the CACNA1A gene T666M mutation: a description of 5 families with familial hemiplegic migraine. *Arch. Neurol.* **60**:684–688.
  83. Curtain, R.P., Smith, R.L., Ovcaric, M., and Griffiths, L.R. 2006. Minor head trauma-induced sporadic hemiplegic migraine coma. *Pediatr. Neurol.* **34**:329–332.
  84. Lakso, M., et al. 1996. Efficient in vivo manipulation of mouse genomic sequences at the zygote stage. *Proc. Natl. Acad. Sci. U. S. A.* **93**:5860–5865.
  85. Nomura, M., McKenna, E., Korach, K.S., Pfaff, D.W., and Ogawa, S. 2002. Estrogen receptor-beta regulates transcript levels for oxytocin and arginine vasopressin in the hypothalamic paraventricular nucleus of male mice. *Brain Res. Mol. Brain Res.*



- 109:84–94.
86. Sullivan, T.R., Jr., et al. 1995. Estrogen inhibits the response-to-injury in a mouse carotid artery model. *J. Clin. Invest.* **96**:2482–2488.
87. Bergman, M.D., et al. 1992. Up-regulation of the uterine estrogen receptor and its messenger ribonucleic acid during the mouse estrous cycle: the role of estradiol. *Endocrinology.* **130**:1923–1930.
88. Horsburgh, K., Macrae, I.M., and Carswell, H. 2002. Estrogen is neuroprotective via an apolipoprotein E-dependent mechanism in a mouse model of global ischemia. *J. Cereb. Blood Flow Metab.* **22**:1189–1195.
89. Becker, J.B., et al. 2005. Strategies and methods for research on sex differences in brain and behavior. *Endocrinology.* **146**:1650–1673.
90. Felicio, L.S., Nelson, J.F., and Finch, C.E. 1980. Spontaneous pituitary tumorigenesis and plasma oestradiol in ageing female C57BL/6J mice. *Exp. Gerontol.* **15**:139–143.
91. Sherman, B.M., West, J.H., and Korenman, S.G. 1976. The menopausal transition: analysis of LH, FSH, estradiol, and progesterone concentrations during menstrual cycles of older women. *J. Clin. Endocrinol. Metab.* **42**:629–636.
92. Nelson, J.F., Felicio, L.S., Osterburg, H.H., and Finch, C.E. 1981. Altered profiles of estradiol and progesterone associated with prolonged estrous cycles and persistent vaginal cornification in aging C57BL/6J mice. *Biol. Reprod.* **24**:784–794.
93. Belisle, S., and Lehoux, J.G. 1983. Endocrine aging in C57 BL mice – II. Dynamics of estrogen receptors in the hypothalamic-pituitary axis. *J. Steroid Biochem.* **18**:737–743.
94. Belisle, S., Bellabarba, D., and Lehoux, J.G. 1985. Age-dependent, ovary-independent decrease in the nuclear binding kinetics of estrogen receptors in the brain of the C57BL/6J mouse. *Am. J. Obstet. Gynecol.* **153**:394–401.
95. Strathy, J.H., Coulam, C.B., and Spelsberg, T.C. 1982. Comparison of estrogen receptors in human premenopausal and postmenopausal uteri: indication of biologically inactive receptor in postmenopausal uteri. *Am. J. Obstet. Gynecol.* **142**:372–382.
96. Tureyen, K., et al. 2007. Peroxisome proliferator-activated receptor-gamma agonists induce neuroprotection following transient focal ischemia in normotensive, normoglycemic as well as hypertensive and type-2 diabetic rodents. *J. Neurochem.* **101**:41–56.
97. Beckman, J.S., Parks, D.A., Pearson, J.D., Marshall, P.A., and Freeman, B.A. 1989. A sensitive fluorometric assay for measuring xanthine dehydrogenase and oxidase in tissues. *Free Radic. Biol. Med.* **6**:607–615.